Washington, D. C.
‡Submitted in partial fulfillment of the requirements for the Ph. D. degree at The Catholic University of America, Washington, D. C.
[1]M. H. Cohen, M. J. Harrison, and W. A. Harrison, Phys. Rev. 117, 937 (1960).
[2]H. J. Foster and P. H. E. Meijer, Natl. Bur. Std. J. Res. 71A, 127 (1967).
[3]L. Flax and J. Trivisonno, Phys. Letters 22, 569 (1966).
[4]J. R. Peverley, Phys. Rev. 173, 689 (1968).
[5]See, for example, H. M. Rosenberg, *Low Temperature Solid State Physics* (Oxford U. P., Oxford, England, 1963), p. 94.
[6]D. K. C. MacDonald, G. K. White, and S. B. Woods, Proc. Roy. Soc. (London) A235, 358 (1956).
[7]G. G. Natale and I. Rudnick, Phys. Rev. 167, 687 (1968).
[8]C. P. Bean, R. W. deBlois, and L. B. Nesbitt, J. Appl. Phys. 30, 1976 (1959).
[9]R. A. Young, Phys. Rev. 175, 813 (1968).
[10]A. Hasegawa, J. Phys. Soc. Japan 19, 504 (1964).
[11]R. G. Chambers, in *Solid State Physics* (Gordon and Breach, New York, 1968), pp. 310–321.
[12]See, for example J. M. Ziman, *Principles of the Theory of Solids* (Cambridge U. P. Oxford, England, 1964), p. 184.
[13]A. B. Pippard, Phil. Mag. 46, 1107 (1955).
[14]A. B. Pippard, Proc. Roy. Soc. (London) 305A, 291 (1968).

PHYSICAL REVIEW B VOLUME 2, NUMBER 8 15 OCTOBER 1970

Modulated Piezoreflectance in Bismuth†

P. Y. Wang* and A. L. Jain
Department of Electrical Engineering, University of Nebraska, Lincoln, Nebraska 68508
(Received 21 May 1970)

Piezoreflectance has been measured in single crystals of bismuth with light polarized in the basal plane of the crystal for photon energies in the range 0.6 to 4.5 eV. The stress modulation of the optical reflectance was achieved by cementing a nearly circular disk of bismuth onto a lead-zirconate-titanate disk set into radial oscillations at 22 kcps. Using the Kramers-Kronig analysis, the induced changes in the imaginary part of the basal component of the dielectric tensor ϵ_{ij} have been computed from the piezoreflectance data. The energy dependence of the piezoreflectance $(\Delta R/R)_{11}$, as well as the computed changes in the dielectric constant $\Delta\epsilon_{11}'$, show an enhancement of the structure observed earlier by Cardona and Greenaway in the reflectivity spectrum. An assignment of the optical structure to direct interband transitions has been possible with the help of a comparison of the data with Golin's band-structure calculations.

INTRODUCTION

The electronic energy band structure of bismuth has been extensively investigated using the well-known experimental methods[1] of the de Haas–van Alphen effect, cyclotron resonance, magnetoacoustic attenuation, far-infrared absorption, magnetoreflection, and the various galvanomagnetic effects The results of all these experiments are in agreement with the two-overlapping-band model, [2–5] in which the Fermi surface for electrons in bismuth consists of three equivalent approximate ellipsoids in momentum space located at the symmetry points L in the Brillouin zone, and that for holes is a single ellipsoid of revolution located at the point T (Fig. 1). Using the two-band model, the experimental values of the direct energy gap at the point L, and the energy overlap between the conduction band and the valence band have been determined[4,6] to be $E_g = 15.3$ meV and $E_0 = 38.5$ meV, respectively. Starting with the Lin-Kleinman pseudopotential, [7] Golin[8] has determined its parameters for bismuth by adjusting to these experimentally determined values of E_g and E_0, and has then calculated the electronic energies of the various bands along several symmetry lines and planes. Although these calculations estimate the effective masses of electrons and holes to be approximately three times larger than the experimental values, the calculated direct interband energies are in agreement with the photon energies which give rise to peaks in the orbital reflectivity spectrum of bismuth.[9] Mase[10] and Ferreira[11] have also calculated the band structure of bismuth using the tight-binding and the augmented-plane-wave (APW) methods, respectively.

Recently interband transitions in solids have been determined by means of electric field, [12–14] temperature, [15,16] and stress[17–19] modulation of the optical reflectivity and absorption. It is well known now that the structure in the photon energy dependence of the imaginary part of the dielectric constant is considerably enhanced by such modulation

techniques.[20] In the present work, we have made extensive measurements of the piezoreflectance in bismuth at near-normal incidence in the energy range 0.6–4.5 eV, and with the help of the Kramers-Kronig analysis determined several critical-point energies. On the basis of a detailed comparison with the published band-structure calculations, the experimental values of the critical-point energies are found to be in agreement with those obtained by pseudopotential method.[8]

EXPERIMENTAL DETAILS

Large bismuth crystals were grown in a horizontal furnace using zone-refined 99.9999% purity material purchased from consolidated Mining and Smelting Co. of Canada. Several single-crystal disks, having approximate dimensions of 1 cm. diam and 2 mm thick, were obtained by cleaving at liquid-nitrogen temperature and mechanically grinding the back surface. In order to obtain a mirror finish on the front surface, the cleaved surface was mechanically polished with 0.05-μ Al_2O_3 powder, and subsequently, electropolished using a solution of 140 g of potassium iodide and 0.4 liter of hydrochloric acid in 0.8 liter of distilled water. Finally, the samples were rinsed with 50% HCl–50% alcohol solution and distilled water. The electropolishing removes the surface damage produced by mechanical polishing. To determine when this damage is removed, Laue patterns were taken at various stages of electropolishing. Because of the high atomic number of bismuth, the Laue method is very sensitive to the presence of surface damage.

The stress modulation of the optical properties was achieved by cementing one of the bismuth disks having its normal along the trigonal axis on a lead-zirconate-titanate (PZT-4) disks of 4 in. diam and 0.25 in. thick with Epoxy resin. The PZT-4 disks was set into radial oscillations at its resonant frequency of 22 kHz. In order to reduce the pickup of any undesirable signals at 22 kHz, the PZT along with the bismuth sample, was mounted in a well-shielded metallic box which was also acoustically insulated from the rest of the experimental setup. From the measured voltage of the 22-kHz signal, the piezoelectric coefficients, and the mechanical Q of the PZT disk, the rms values of the stress components in the basal plane were estimated to be $\sigma_{11}=\sigma_{22}\simeq 1.2\times10^{8}$ dyn/cm^2, where the subscripts 1, 2, and 3 are used to denote the binary, bisectrix, and trigonal axes, respectively. Using room-temperature elastic-constant data,[21] the rms values of the corresponding strain components are calculated to be $e_{11}=e_{22}\simeq 2.5\times10^{-4}$ and $e_{33}\simeq -2.7\times10^{-4}$.

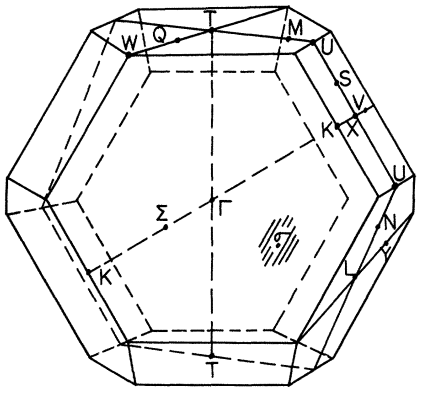

FIG. 1. The Brillouin zone for Bismuth (reproduced from Ref. 8).

The modulated piezoreflectance was measured by conventional techniques. Light from a high-pressure 150-W xenon arc lamp was passed through a model 98 Perkin-Elmer prism monochromator. The monochromatic beam was polarized normal to the plane of incidence by a Glan-Thompson prism and was incident on the basal plane of the bismuth sample at an angle of ~5°. The dc and ac components in the reflected light were measured with the help of RCA 1P28 or thermoelectrically cooled 7102 photomultiplier tubes, a dc vacuum-tube voltmeter, and a Princeton Applied Research HR-8 lock-in amplifier. The piezoreflectance $(\Delta R/R)_{11}$ was obtained from the ratio of the ac-to-dc signals over a range of photon energies from 0.6 to 4.5 eV.

EXPERIMENTAL RESULTS

The optical properties of a trigonal crystal are determined by the complex second-rank tensor ϵ_{ij} which has two independent components denoted by $\epsilon_{11}=\epsilon_{22}$ and ϵ_{33} in the coordinate system in which subscript 1, 2, and 3 are used to denote the binary, bisectrix, and trigonal axes, respectively. With the stress applied radially in the basal plane of the bismuth crystal, the piezoreflectance $(\Delta R/R)_{11}$ for the light polarized along the basal plane can be expressed as

$$\left(\frac{\Delta R}{R}\right)_{11}=\frac{\partial \ln R_{11}}{\partial \epsilon'_{11}}\,\Delta\epsilon'_{11}+\frac{\partial \ln R_{11}}{\partial \epsilon''_{11}}\,\Delta\epsilon''_{11}\cdots , \quad (1)$$

where ϵ'_{11} and ϵ''_{11} are the real and the imaginary parts of the basal component of the dielectric tensor ϵ_{ij}.

In order to determine the changes $\Delta\epsilon'_{11}$ and $\Delta\epsilon''_{11}$, we have first calculated the induced changes in the phase angle $\Delta\theta$ using the Kramers-Kronig relation

$$\Delta\theta=\frac{1}{2\pi}\int_0^\infty \frac{d}{dw'}\left(\frac{\Delta R}{R}\right)\ln\left|\frac{w'+w}{w'-w}\right| dw'\cdots , \quad (2)$$

where, in order to carry out the numerical integra-

tion, the measured values of $(\Delta R/R)_{11}$ have been used for the energy range 0.6–4.5 eV, while outside this range, $(\Delta R/R)_{11}$ has been assumed to be zero. From the values of $(\Delta R/R)_{11}$ and $\Delta\theta$, $\Delta\epsilon'_{11}$ and $\Delta\epsilon''_{11}$ have been calculated using the relations

$$\Delta\epsilon'_{11}=\tfrac{1}{2}A(\Delta R/R)_{11}+B(\Delta\theta)_{11}\,,$$
$$\Delta\epsilon''_{11}=\tfrac{1}{2}B(\Delta R/R)_{11}-A(\Delta\theta)_{11}\cdots\,, \tag{3}$$

where

$$A=n_{11}(\epsilon'_{11}-1)-k_{11}\epsilon''_{11}\,,\quad B=k_{11}(\epsilon'_{11}-1)+n_{11}\epsilon''_{11}\,.$$

The optical constants n_{11} and k_{11} were taken from the measurements of Lenham, Treherne, and Metcalfe.[22] The values of these constants compare favorably with the results obtained by ellipsometry on the samples used in the present work assuming an isotropic dielectric tensor. In Fig. 2, the optical-constant data of Lenham, Treherne, and Metcalfe have been reproduced along with the present ellipsometric measurements. The measured piezoreflectance $(\Delta R/R)_{11}$ and the computed $(\Delta\theta)_{11}$, $\Delta\epsilon'_{11}$, and $\Delta\epsilon''_{11}$ are shown in Figs. 3 and 4 as a function of photon energy in the range 0.6–4.5 eV. As can be seen from these figures, the stress modulation considerably enhances the optical structure as compared to the unmodulated optical studies. The various energies at which sharp peaks appear in $(\Delta R/R)_{11}$ and $\Delta\epsilon''_{11}$ spectra are presented in Table I along with the energies at which peaks were observed in the reflectivity spectrum.[9]

Experimental uncertainties in the energy values in Table I are at most ±0.01 eV in the visible and ±0.02 eV in the infrared regions.

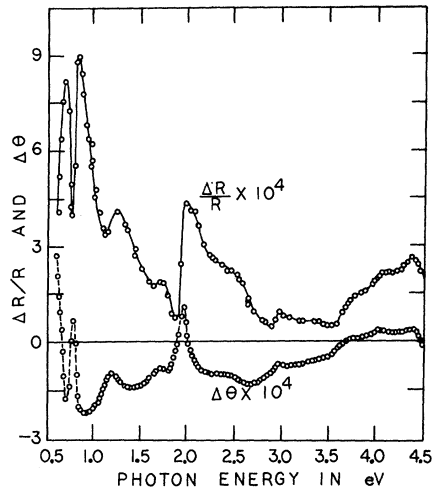

FIG. 3. Piezoreflectance $(\Delta R/R)_{11}$ and the change in the phase angle $(\Delta\theta)_{11}$ calculated using Kramers-Kronig relation.

INTERPRETATION AND DISCUSSION

According to the deformation potential theory, the energies of the electron bands are shifted in proportion to the strain. Consequently, changes in the critical-point energies caused by the strains e_{11}, e_{22}, and e_{33}, can be expressed as

$$\Delta w_g = E_{11}(e_{11}+e_{22})+E_{33}e_{33}\cdots\,, \tag{4}$$

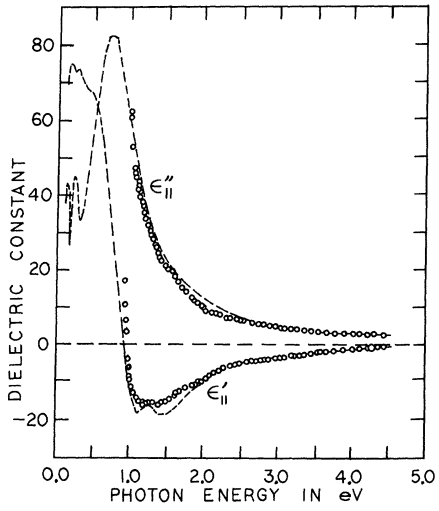

FIG. 2. Real and imaginary parts of the dielectric constant measured by ellipsometry are shown as circles, and those by Lenham, Treherne, and Metcalf are shown as dashed lines.

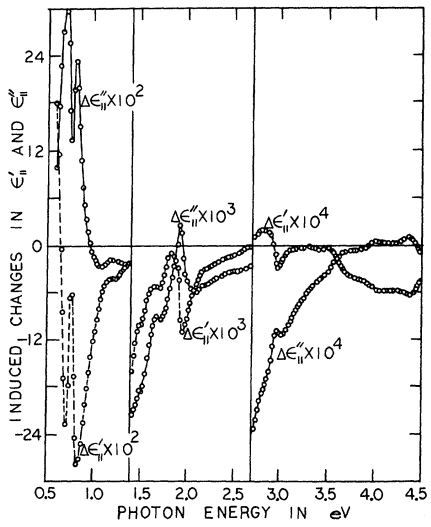

FIG. 4. Stress induced changes in the real and the imaginary parts of the dielectric component ϵ_{11} shown as a function of photon energy.

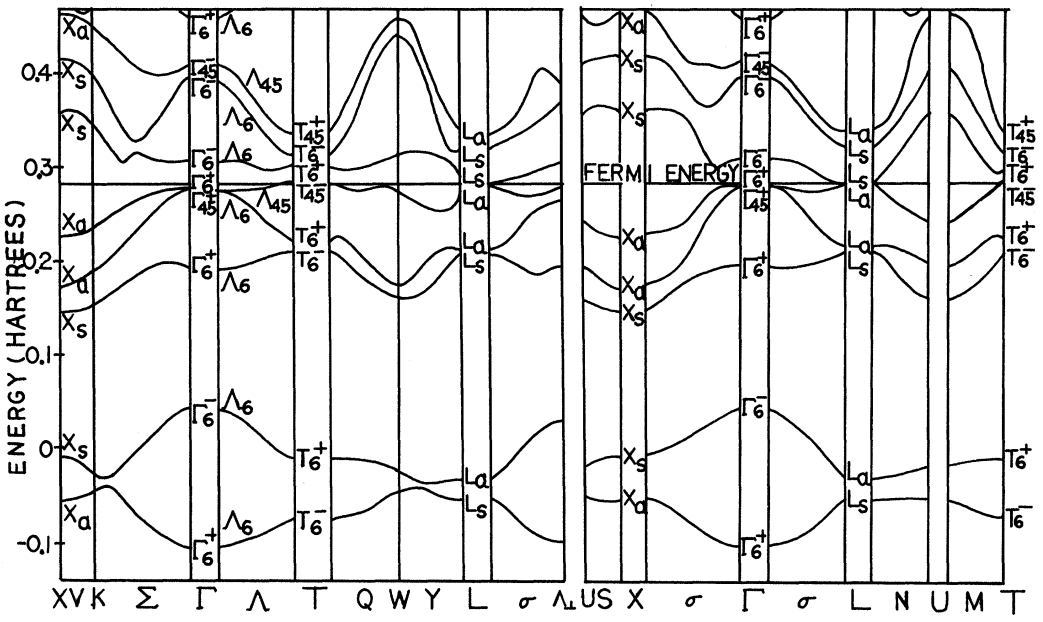

FIG. 5. Pseudopotential band-structure calculations of bismuth reproduced from Ref. 8.

where E_{11} and E_{33} are the deformation potential constants representing the changes in the critical-point energies per unit strain. The energy shifts Δw_g, in turn, lead to the changes in the real and the imaginary parts of the dielectric tensor components, which for the special case of radial stress applied in the basal plane, and the light also polarized in the same plane, are given by

$$\frac{\partial \epsilon_{11}}{\partial e_{11}} = \frac{\partial \epsilon_{11}}{\partial w_g} E_{11} \cdots , \quad \text{and} \quad \frac{\partial \epsilon_{11}}{\partial e_{33}} = \frac{\partial \epsilon_{11}}{\partial w_g} E_{33} . \qquad (5)$$

In order to determine E_{11} and E_{33}, we would require, in addition to the present experimental results, measurements of the changes in the optical reflectivity induced by hydrostatic pressure. Since appropriate reflectivity data at high pressures are not available, we have neglected the contribution of e_{33} to Δw_g, computed $d\epsilon_{11}''/dw_g$ from the optical-constants data (Fig. 2), and have finally arrived at $E_{11} \sim -1$ eV for the critical-point energy of 1.92 eV. Similar order-of-magnitude values for the deformation potential constants[23,24] in bismuth have been estimated for the indirect interband energy involving the overlapping conduction and valence bands at the points L and T of the Brillouin zone.

The assignment of the various peaks observed in the piezoreflectance spectrum and $\Delta\epsilon_{11}''$ has been accomplished by comparing the energies of the observed peaks in the spectrum with the predicted critical-point energies in the band-structure calculations. As can be seen from Table I, the present experimental results are in excellent agreement with the pseudopotential calculations performed by adjusting the pseudopotential parameters such that there is a good agreement between the experimental and the theoretical values of the smallest energy gap at the point L and the energy overlap between the conduction and the valence bands. These values, determined from magneto-optical reflection[4] and the Shubinkov–de Haas effect[6] at liquid-helium temperature, are known to be

$$E_g = E[L_s(3)] - E[L_a(3)] = 15.3 \times 10^{-3} \text{ eV} ,$$

$$E_0 = E[T_{45}^-(1)] - E[L_s(3)] = 38.5 \times 10^{-3} \text{ eV} .$$

All the experiments aimed at determining the nature of charge carriers in bismuth are in accord with this overlapping-band model.

Since in the present experiment incident light is polarized along the basal plane, we do not expect any interband transitions at the point T in $\vec{k}$ space. In the lower-energy region of the spectrum (Figs. 3 and 4), two very strong peaks are observed at the photon energies of 0.69 and 0.81 eV. At the same energies, Lenham, Treherne, and Metcalfe have observed a peaked behavior in the basal component ϵ_{11}'' (reproduced in Fig. 2). Comparing these energies with the pseudopotential calculations (Fig. 5 reproduced from Ref. 9), we assign them to the $\Gamma_6^+(3) \rightarrow \Gamma_6^-(2)$ and the $\Gamma_{45}^+(1) \rightarrow \Gamma_6^-(2)$ transitions. Furthermore, since these bands are almost flat for $\vec{k}$ in the neighborhood of Γ, the condition $\vec{\nabla}_k(E_m - E_n) = 0$ is satisfied over a large volume of the Brillouin

TABLE I. Interband transition energies and the assignment of the optical structure by comparison with Golin's calculations.

Energy (piezo-reflectance) (eV)	Designation[a] (reflectance)	Energy[b] (pseudo-potential) (eV)	Bands	Locations in Brillouin zone
0.69		0.821	5→6	$\Gamma_6^+(3) \rightarrow \Gamma_6^-(2)$
0.81		0.825	4→6	$\Gamma_{45}^+(1) \rightarrow \Gamma_6^-(2)$
1.15	E_1(1.2 eV)	1.133	5→7	$L_a(3) \rightarrow L_s(4)$
1.68	E_2(1.7 eV)	1.530	6→8	$L_s(3) \rightarrow L_a(4)$
1.92		1.826	4→6	$L_a(2) \rightarrow L_s(3)$
2.49		2.480	5→7	near Σ
		2.510	4→7	near Λ
2.96	E_3(3.1 eV)	2.943	4→7	$L_a(2) \rightarrow L_s(4)$
3.33		3.196	4→7	$\Gamma_{45}^+(1) \rightarrow \Gamma_6^-(3)$
		3.192	5→7	$\Gamma_6^+(3) \rightarrow \Gamma_6^-(2)$
3.57		3.407	3→8	$L_s(2) \rightarrow L_a(4)$
		3.623	4→8	$\Gamma_{45}^+(1) \rightarrow \Gamma_{45}^-(1)$
		3.619	5→8	$\Gamma_6^+(3) \rightarrow \Gamma_{45}^-(1)$
		3.597	5→6	$X_a(3) \rightarrow X_s(3)$
4.00				
4.38				

[a]See Ref. 9. [b]See Ref. 8.

zone and, consequently, is responsible for a large contribution to ϵ_{11}''; which is in accord with the observed peaked behavior in ϵ_{11}'' at 0.69 and 0.81 eV. The general shape of the unmodulated optical spectrum suggests these critical points to be of M_1 and M_2 types, respectively.

In the energy range 1–2 eV there are three well-pronounced peaks at 1.15, 1.68, and 1.92 eV. The peak at 1.15 eV is in agreement with the 1.2-eV peak observed by Cardona and Greenaway, and is in agreement with the transition 5→7 at the point L designated $L_a(3) \rightarrow L_s(4)$ by Golin. In the previously published optical data, a peak in the optical reflectivity and some weak structure in ϵ_{11}'' were observed in the energy range 1.5–2 eV. This structure is considerably enhanced by the piezomodulation technique, and the two peaks at 1.68 and 1.92 eV could be assigned to 6→8 and 4→6 interband transitions at the symmetry point L and designated $L_s(3) \rightarrow L_a(4)$ and $L_a(2) \rightarrow L_s(3)$, respectively. Since $L_s(3)$ is the conduction band in bismuth, the contribution to ϵ_{11}' and ϵ_{11}'' due to these transitions is likely to be sensitive to the temperature and to the small concentration of impurities present in the sample.

Compared to the electronic transitions in the longer-wavelength region, the transitions at energies >2 eV are several times weaker. There is considerable structure in the piezoreflectance spectrum which is further weakened in $\Delta\epsilon_{11}''$, partly owing to the smaller values of coefficients A and B in the shorter-wave length region and partly owing to the use of the Kramers-Kronig relation. In the piezoreflectance spectrum, weak peaks are observed at 2.49, 2.96, 3.33, 3.57, 4.00, and 4.38 eV. The various possible electronic transitions which could give rise to these peaks are shown in Table I. According to the pseudopotential calculations, the 2.96-eV transition can be ascribed to $L_a(2) \rightarrow L_s(4)$. For the rest of the transitions there are several possible assignments at the symmetry points X and Γ of the Brillouin zone.

ACKNOWLEDGMENTS

Thanks are extended to Dr. A. P. Lenham for sending us the numerical values of their optical data, and to K. Dykes for the assistance provided in the experimental set up and much useful discussion during the course of this work.

†Work supported in part by a grant from the National Science Foundation.

*Parts of the work submitted in partial fulfillment of the requirements for the Ph.D. degree.

[1]For extensive bibliographics see, W. S. Boyle and G. E. Smith, Progr. Semicond. 7, 1 (1963); IBM J. Res. Develop. 8, 215 (1964); R. N. Bhargava, Phys. Rev. 156, 785 (1967).

[2]M. H. Cohen, Phys. Rev. 121, 387 (1961).

[3]A. L. Jain and S. H. Koenig, Phys. Rev. 127, 442 (1962).

[4]R. N. Brown, J. G. Mavroides, and B. Lax, Phys. Rev. 129, 2055 (1963).

[5]S. H. Koenig, A. A. Lopez, D. B. Smith, and J. L. Yarnell, Phys. Rev. Letters 20, 48 (1968).

[6]G. E. Smith, G. A. Baraff, and J. M. Rowell, Phys. Rev. 135, A1118 (1964).

[7]P. J. Lin and L. Kleinman, Phys. Rev. 142, 478 (1966).

[8]S. Golin, Phys. Rev. 166, 643 (1968).

[9]M. Cardona and D. L. Greenaway, Phys. Rev. 133, A1685 (1964).

[10]S. Mase, J. Phys. Soc. Japan 14, 584 (1959).

[11]L. G. Ferreira, J. Phys. Chem. Solids 28, 1891 (1967); 29, 357 (1968).

[12]B. O. Seraphin and R. B. Hess, Phys. Rev. Letters 14, 138 (1965).

[13]M. Cardona, K. L. Shaklee, and F. H. Pollak, Phys. Rev. 154, 696 (1967).

[14]A. Frova, P. Handler, F. Germano, and D. E. Aspnes, Phys. Rev. 145, 575 (1966).

[15]B. Batz, Solid State Commun. 4, 241 (1966); 5, 985 (1967).

[16]E. Matatagui, A. Thompson, and M. Cardona, Phys. Rev. 176, 950 (1968).

[17]W. Engeler, H. Fritzsche, M. Garfinkel, and J. J. Tiemann, Phys. Rev. Letters 14, 1069 (1965).

[18]U. Gerhardt, D. Beaglehole, and R. Sandrock, Phys. Rev. Letters 19, 309 (1967).

[19]I. Balsev, Solid State Commun. 5, 315 (1967).

[20]For extensive bibliographies, see M. Cardona, *Modulation Spectroscopy* (Academic, New York, 1969).
[21]Y. Eckstein, A. W. Lawson, and D. H. Reneker, J. Appl. Phys. 31, 1534 (1960).
[22]A. P. Lenham, D. M. Treherne, and R. J. Metcalfe, J. Opt. Soc. Am. 55, 1072 (1965).
[23]A. L. Jain and R. Jaggi, Phys. Rev. 135, A708 (1964).
[24]K. Walther, Phys. Rev. 174, 782 (1968).

PHYSICAL REVIEW B VOLUME 2, NUMBER 8 15 OCTOBER 1970

Lattice Dynamics of Alkali Metals in the Self-Consistent Screening Theory*

D. L. Price
Argonne National Laboratory, Argonne, Illinois 60439
and
K. S. Singwi
Northwestern University, Evanston, Illinois 60204
and Argonne National Laboratory, Argonne, Illinois 60439
and
M. P. Tosi
Argonne National Laboratory, Argonne, Illinois 60439
and Department of Physics, University of Messina, Italy
(Received 27 April 1970)

The self-consistent treatment of correlations in the electron liquid recently given by Singwi *et al.* is applied to calculations of the lattice dynamics of alkali metals. With the Ashcroft form for the pseudopotential, in which the only parameter is the core radius, good agreement with the measured dispersion curves is obtained for the four metals for which such data exist. For Na and K the fitted values of this parameter are close to those derived from Fermi-surface and liquid-resistivity data; for Li and Rb the fitted values lie between those obtained from the other physical properties. Phonon lifetimes due to the electron-phonon interaction are calculated for K. Finally, the cohesive energy, lattice parameter, and compressibility are derived; agreement with the measured values of all three quantities is obtained with a not unreasonable adjustment of the Hartree energy. The relation between the compressibility sum rule and the long-wavelength limit of terms containing third and fourth powers of the electron-phonon matrix element is evaluated for the case of Na within the same framework.

I. INTRODUCTION

Since the pioneering work of Toya,[1] there have been many attempts to calculate phonon dispersion relations in the alkali metals starting from first principles. Such work has been stimulated by the experimental data from inelastic neutron scattering[2-5] and also by the development of pseudopotential theory[6] which has largely justified, at least for the alkali metals, Toya's use of plane-wave states to derive the electron-phonon matrix elements. The essential ingredients of these calculations are the form of the pseudopotential and the treatment of the screening. The calculations published hitherto[7-16] have used a variety of forms for the pseudopotential, including Bardeen's,[1,8,9,15] different types of self-consistent orthogonalized-plane-wave (OPW) calculation,[7,8,15,16] the Heine-Abarenkov model potential fitted to atomic spectroscopic data,[10] and parametrized forms such as those suggested by Schneider and Stoll,[11] by Ashcroft,[12] by Brovman *et al.*,[13] and by Harrison.[14] Different forms of screening have been used also, ranging from simple Hartree screening random-phase approximation (RPA)[8,10,15] to more complicated forms incorporating exchange and correlation effects, such as Slater's,[1,15] Hubbard's modified form[7,8,10,15] and those of Bailyn,[9] Kohn and Sham,[15] Robinson *et al.*,[15] Geldart and Vosko,[8,11-15] and Geldart and Taylor.[16] Most authors assume a local pseudopotential, although several attempts have been made to include nonlocal corrections.[7,8,10] Most of the calculations are taken to second order in the electron-ion matrix element; while two groups have discussed the formalism for carrying the calculations to higher order,[17,18] no results are available at the time of writing.

The frequencies are generally within 10 to 20% of the observed ones for the first-principles calculations, somewhat closer for those containing adjustable parameters. The physical information derived